Accepted Manuscript

Monitoring WWTP performance using size-exclusion chromatography with simultaneous UV and fluorescence detection to track recalcitrant wastewater fractions

Alexey Ignatev, Tuula Tuhkanen

PII: S0045-6535(18)31754-5

DOI: 10.1016/j.chemosphere.2018.09.099

Reference: CHEM 22179

To appear in: *ECSN*

Received Date: 21 April 2018

Revised Date: 12 September 2018

Accepted Date: 17 September 2018

Please cite this article as: Ignatev, A., Tuhkanen, T., Monitoring WWTP performance using size-exclusion chromatography with simultaneous UV and fluorescence detection to track recalcitrant wastewater fractions, *Chemosphere* (2018), doi: https://doi.org/10.1016/j.chemosphere.2018.09.099.

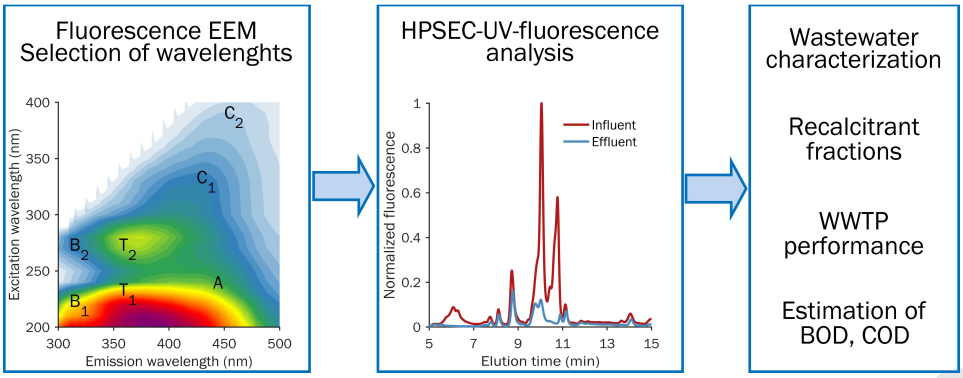

Monitoring WWTP performance using size-exclusion chromatography with simultaneous UV and fluorescence detection to track recalcitrant wastewater fractions

Alexey Ignatev*, Tuula Tuhkanen

Department of Biological and Environmental Science, University of Jyväskylä, PO Box 35, FI-40014, Jyväskylä, Finland

* Corresponding author

E-mail addresses:

alexey.n.ignatev@jyu.fi, alexignat@gmail.com (A. Ignatev),

tuula.a.tuhkanen@jyu.fi (T. Tuhkanen).

Abstract

A trial monitoring of a typical full-scale municipal WWTP in Central Finland was aimed to explore applicability of high performance liquid chromatography – size exclusion chromatography (HPSEC) with simultaneous UV and fluorescence detection as a tool for advanced routine monitoring of wastewater treatment. High, intermediate, and low molecular weight (MW) fractions of wastewater influent and secondary effluent were characterized in terms of UV absorbance at 254 nm (UVA_{254}) and specific fluorescence represented tyrosine-like, tryptophan-like, and humic/fulvic-like compounds.

The activated sludge treatment removed 97 ± 1% of BOD, 93 ± 2% of COD, 71 ± 7% of DOC, and 24 ± 7% of TN, while reduction of total UVA_{254} was 50 ± 6%. Intensity of total fluorescence signal declined by ~80% for tyrosine-like, by 60-70% for tryptophan-like, and by 7-36% for humic/fulvic-like compounds. Low and intermediate MW humic/fulvic-like compounds fluorescing at $\lambda_{ex}/\lambda_{em}$ = 390/500 nm demonstrated recalcitrant behavior. Protein-like and humic/fulvic-like fractions of low MW < 1 kDa accounted for 60-65% of total UVA_{254} and 50-70% of total fluorescence of whole influent and effluent samples. Strong linear correlations were observed between BOD, COD, DOC, UVA_{254} and tyrosine-like, tryptophan-like fluorescence.

The analytical approach based on HPSEC with simultaneous UV and fluorescence detection allows rapid and advanced characterization of natural and anthropogenic organic matter in water treatment and distribution systems. Fairly good resolution archived in the HPSEC separation offers new opportunities for fingerprinting and tracking specific wastewater fractions.

Keywords

Wastewater treatment;
Wastewater characterization;
Size-exclusion chromatography;
UV absorption;
Fluorescence;
Molecular weight distribution.

1. Introduction

In recent years, diverse contamination of the aquatic environment has been recognized by governmental regulators as a challenging and pervasive issue. The European Commission demands a strategic approach to control water pollution and calls for development of advanced but affordable analytical tools for routing monitoring (Directive, 2013). Of rising concern is current situation with emerging pollutants, which are not included in ongoing monitoring programs, but could pose significant risk (Directive, 2013).

In Europe, 95% of urban wastewater is collected and over 85% is treated according to the official requirements (Directive, 1991; European Commission, 2017). However, conventional wastewater treatment plants (WWTPs) incompletely remove emerging pollutants present at low concentrations, moreover, some soluble microbial products (SMPs) formed in activated sludge are more toxic and/or mutagenic than their parent compounds (Shon et al., 2006b). Thus, WWTPs become point sources of complex contamination of receiving water bodies. Importance of this issue rises in the light of water reuse. For example, Cyprus currently reuses 97% of treated wastewater (European Commission, 2017).

Performance of WWTPs and quality of wastewater effluent discharges are routinely assessed in terms of chemical and biochemical oxygen demand (COD and BOD), dissolved organic carbon (DOC), total nitrogen (TN), UV absorbance at 254 nm (UVA_{254}), etc. However, these parameters are indicative and do not provide detailed information on properties of specific components of dissolved organic matter (DOM). At the same time, additional information is needed for contamination source tracking, designing and optimizing post-treatment, and risk assessment, particularly, due to impact of DOM on bioavailability of pollutants and xenobiotics (Choudhry, 1983).

While comprehensive characterization of DOM requires multi-method analytical approach (Abbt-Braun et al., 2004), many advanced techniques have limited applicability for routine monitoring of wastewater. For example, nuclear magnetic resonance (NMR) and pyrolysis-gas chromatography-mass spectrometry (py-GC/MS), being sensitive and powerful for structural analysis, are laborious, expensive, and require considerable operator expertise (Her et al., 2003).

Moreover, multicomponent polyfunctional nature of wastewater results in tangled NMR spectra and pyrochromatograms that are hard to interpret (Sillanpää et al., 2015).

Over the last decade, fluorescence spectroscopy has gained significant attention as a sensitive and inexpensive technique to control and optimize wastewater treatment (Carstea et al., 2016; Henderson et al., 2009; Mesquita et al., 2017). Rapid development is happening in the field of fluorescence sensors for online monitoring (Li et al., 2016). Due to high selectivity and sensitivity fluorescence detection can complement robust but limited UV-Vis spectroscopy.

Whole wastewater samples are often analyzed using excitation-emission matrix (EEM) fluorescence spectroscopy, which covers a wide range of excitation and emission wavelengths ($\lambda_{ex}/\lambda_{em}$), usually, from ~200 to ~500 nm. Interpretation of EEM spectra via peak-picking, regional integration, parallel factor analysis (PARAFAC), in principle, allows discriminating different types of DOM from natural and anthropogenic sources (Chen et al., 2003; Yang et al., 2015). However, mitigation of the inner-filtering in samples with high DOC content requires additional steps: controlled dilution (Henderson et al., 2009) and/or algebraic correction (Kothawala et al., 2013). Shifting, overlapping, and broadening of peaks complicate EEM analysis (Yang et al., 2015). PARAFAC mathematically decomposes EEM spectra into simulated fluorescing components that are independent spectrally, but not necessarily physicochemically (Li et al., 2014). It leads to inconsistencies across EEM-PARAFAC studies (Ishii and Boyer, 2012).

Many of the aforementioned issues are avoided in high performance liquid chromatography – size-exclusion chromatography (HPSEC), which is widely used to characterize DOM in raw and drinking water (Sillanpää et al., 2015) and also in wastewater (Chon et al., 2017; Guo et al., 2011; Her et al., 2003; Imai et al., 2002; Jarusutthirak and Amy, 2007; Nam and Amy, 2008; Shon et al., 2006a, 2004; Szabo et al., 2016; Yan et al., 2012). HPSEC separates DOM components according to their molecular weight (MW) into fractions. In absence of secondary interactions, longer elution time corresponds to smaller MW. Secondary interactions, such as adsorption on the column material, hydrophobic and electrostatic effects, lead to advanced or delayed elution that violates the mechanism of purely steric exclusion (Le Coupannec et al., 2000). While hydrophobic effects are important at high ionic strength of eluent,

the role of electrostatic effects (particularly, ion exclusion) increases with decrease of eluent ionic strength (Specht and Frimmel, 2000). Eluents of low ionic strength (2-20 mM) provide high chromatographic resolution for anionic compounds, however, elution of cationic compounds is delayed due to the ion exclusion (Le Coupannec et al., 2000). Eluents with high ionic strength may be undesirable because "macromolecule aggregation in wastewater will be destroyed with the addition of Na^+, which can substitute divalent metal ions (such as Ca^{2+}) involved in extracellular polymeric substances bridging" (Guo et al., 2011).

Small sample volume, minimal pre-treatment, ease and speed of the analysis are among practical advantages of HPSEC over other characterization techniques (Michael-Kordatou et al., 2015). In many studies, HPSEC fractionation of wastewater is monitored by UVA_{254} and online DOC, while use of fluorescence detection is less common.

The current work aims to examine applicability of HPSEC with simultaneous UV and fluorescence detection for routine monitoring of WWTP performance and advanced characterization of DOM in wastewater influent and effluent. The object of this study is municipal WWTP Nenäinniemi (Jyväskylä, Finland), operated by Jyväskylän Seudun Puhdistamo Oy. The WWTP serves 155 000 residents, uses a conventional activated sludge treatment and has an average wastewater flow of around 40 000 m^3 day^{-1}, out of which about 13% is produced by local industry. The treated wastewater effluent is discharged into lake Päijänne. No effluent post-treatment was deployed at the time of this study.

2. Materials and methods

2.1. Sampling and sample preparation

All samples of wastewater influent (referred herein as "influent") and the secondary effluent (referred herein as "effluent") were 24 h composite. Preliminary EEM fluorescence analyses were done for one influent and one effluent samples collected on March 19, 2017. During the main sampling campaign samples were collected from the WWTP daily for two weeks, March 26-31 and April 3-6, 2017 (in total, 10 sampling days). To obtain results presented in

Section 3.2.3 additional influent and effluent samples were collected and analyzed in July-September 2017.

Upon delivery to the university laboratory, influent and effluent samples were ultra-centrifuged at 6 000 rpm for 30 min to facilitate further filtration. Additional experiments confirmed that the centrifugation did not affect HPSEC chromatograms. The supernatant was immediately filtered through disposable 0.45 µm cellulose acetate syringe filters (VWR, USA) that were pre-washed with 20 mL of ultrapure water and then air purged. The first few mL of filtrate were discarded.

HPSEC and EEM fluorescence measurements were done within 24 h after sampling. Filtered 20 mL samples for DOC analysis were stored at -20 °C in screw cap polypropylene tubes (Sarstedt, Germany) and analyzed within one month.

2.2. EEM fluorescence spectroscopy

EEM fluorescence spectra of influent and effluent samples were obtained using a Perkin-Elmer SL 55 spectrofluorimeter. The samples were diluted fivefold with ultrapure water. The number of replicates was one.

The excitation interval was 200-500 nm (step 10 nm) and the emission interval was 300-600 nm (step 0.5 nm). The emission cut-off filter was 290 nm, the scan rate was 300 nm min^{-1}, and the slit widths were 10 nm for both excitation and emission. Voltage of the photomultiplier (type R928) was set to “Auto”.

Single emission spectra were combined into EEMs in MATLAB (R2016b, MathWorks, USA). Inner-filtering was corrected algebraically, according to (Kothawala et al., 2013), using UV/Vis spectra obtained with a Shimadzu UV-1800 spectrophotometer. The corrected EEM was normalized by Raman scatter peak of water, as suggested by (Lawaetz and Stedmon, 2009). During data processing, first order Rayleigh light scattering peak, caused by fine colloidal particles, was removed from the EEMs for visual clarity.

2.3. DOC, BOD, and COD

DOC measurements were done using a total organic carbon analyzer Shimadzu TOC-L equipped with an autosampler ASI-L. The non-purgeable organic carbon method was selected.

Neither influent nor effluent samples were diluted. Calibration was done in the DOC range 0-100 mgC L^{-1} using freshly prepared solutions of potassium phthalate. Prior analyses, vials were calcined at 400 °C for 4 h in air. All samples were acidified with HCl and purged with N_2 to strip dissolved inorganic carbon. A single DOC measurement included three 100 µL injections. Two duplicate analyses were done on two different days using two independent calibration curves, and the results were averaged.

BOD (7 days) and COD analyses were done by NabLabs Oy (Jyväskylä, Finland) according to Finnish standards specified in Supplementary material Table S1.

2.4. HPSEC method

Influent and effluent samples were analyzed using an HPLC Shimadzu LC-30AD equipped with online degassing units Shimadzu DGU-20A5R and DGU-20A3R, a column oven Shimadzu CTO-20AC, an autosampler Shimadzu SIL-30AC, a photodiode array (PDA) detector Shimadzu SPD-M20A, and a fluorescence detector Shimadzu RF-20A XS. The column was a silica-based Yarra SEC-3000 (300×7.6 mm, Phenomenex, USA).

An HPSEC method developed for wastewater analysis by (Szabo et al., 2016; Szabo and Tuhkanen, 2010) was adopted after minor modifications. Particularly, sodium acetate eluent was replaced with phosphate buffer to avoid quenching of tyrosine-like fluorescence by acetate ions (Feitelson, 1964). The both eluents demonstrated identical separation in preliminary experiments.

5 mM phosphate buffer with $\beta(Na_2HPO_4 \cdot 2H_2O)$ = 0.45 g L^{-1} and $\beta(NaH_2PO_4 \cdot 2H_2O)$ = 0.39 g L^{-1} (pH 6.8, ionic strength 10 mM) was used as the eluent at a flow rate of 1 mL min^{-1}. Analytical grade $Na_2HPO_4 \cdot 2H_2O$ and $NaH_2PO_4 \cdot 2H_2O$ were purchased from VWR, Belgium, and Merck, Germany, respectively. Ultrapure water was generated using an “Ultra Clear UV plus TM” system (SG Water, Germany). Eluent was pre-filtered through GF/F grade (0.45 µm) cellulose acetate filters (Whatman, Germany).

Neither influent nor effluent samples were diluted for HPSEC analyses. Ionic strength of samples was not adjusted. The injection volume was 15 µL for influent and 30 µL for effluent. The autosampler temperature was 4 °C, and the column oven temperature was 25 °C. Elution

was stopped after 35 min for all the samples. After every 8-10 runs a blank injection of ultrapure water was done to test the column and lines for possible contamination. The HPLC system was regularly flushed with aqueous solutions of HPLC grade methanol or acetonitrile (Merck, Germany) to prevent contamination build-up.

The cell temperature of the PDA detector was 40 °C and the slit width was 1.2 nm. Sensitivity of the fluorescence detector was set to "high", the fluorescence cell temperature was 25 °C, and the response time was 1.5 s. The data acquisition rates were 12.5 Hz and 10.0 Hz for the PDA and the fluorescence detectors, respectively.

The PDA and fluorescence detectors worked in tandem, and a 3D UV spectrum (λ = 200-400 nm vs. elution time) and two fluorescence signals for two different $\lambda_{ex}/\lambda_{em}$ were recorded simultaneously during each chromatographic run. To obtain HPSEC-fluorescence chromatograms for the eight selected $\lambda_{ex}/\lambda_{em}$ each sample was injected four times. Thus, four replicate HPSEC-UV were obtained for each sample, they were averaged during data processing.

Void volume, determined with blue dextran (Sigma-Aldrich, Sweden), was 5.5 mL (elution time 5.5 min), and permeation volume, determined with acetone, was 12.5 mL (elution time 12.5 min). The size-exclusion column was calibrated with polystyrene sulfonate standards of 210, 1 600, 3 200, 4 800, 6 400, 17 000, and 32 000 Da (Sigma-Aldrich, Germany), which are commonly used for HPSEC calibration (Shon et al., 2006a).

2.5. Processing of HPSEC data

Raw chromatographic data were exported from the proprietary software (Shimadzu LabSolutions LC/GC Version 5.51) to ASCII text files and processed in MATLAB using in-house scripts. Each chromatogram was integrated numerically using MATLAB function trapz. Horizontal axis was taken as the baseline, and individual fractions were separated with perpendicular drops.

Total fluorescence and total UVA_{254} were calculated by integration of corresponding chromatograms in the elution time range 4.5–30.0 min. Thus, total fluorescence and total UVA_{254} account for all HPSEC fractions combined and represent properties of whole influent and effluent samples.

In this study, fluorescence and UVA_{254} are expressed in terms of [mV] and [mAU], elution time is given in [min], thus, fractional (and total) fluorescence and UVA_{254} have dimensions of [mV min] and [mAU min], respectively.

Removal efficiencies were calculated according to the following equation

$$Removal\ efficiency = \left(1 - Area_{eff} / Area_{inf}\right) 100\% \quad (1)$$

where $Area_{eff}$ and $Area_{inf}$ are the corresponding areas (total or fractional) of HPSEC chromatograms of influent and effluent sampled on the same day. Removal efficiencies were calculated for each day of the main monitoring period (in total, 10 days) and then were averaged.

Number-averaged MW ($\bar{M}_n$), weight-averaged MW ($\bar{M}_w$), and dispersity ($Đ_M$) were calculated with equations (2)-(4) according to (Her et al., 2002).

$$\bar{M}_n = \sum_{i=1}^{n} h_i \Big/ \sum_{i=1}^{n} \left(h_i / MW_i\right) \quad (2)$$

$$\bar{M}_w = \sum_{i=1}^{n} \left(h_i \cdot MW_i\right) \Big/ \sum_{i=1}^{n} h_i \quad (3)$$

$$Đ_M = \bar{M}_w / \bar{M}_n \quad (4)$$

where h_i and MW_i are the height of HPSEC chromatogram and the estimated MW corresponding to the eluted volume i, and n is the number of data points. The elution time range 4.5-12.5 min was taken to calculate $\bar{M}_w$, $\bar{M}_n$, and $Đ_M$.

UV absorbance ratio index (URI) was calculated as ratio of UVA_{210} to UVA_{254} (Her et al., 2008).

3. Results and discussion

3.1. Analysis of EEM fluorescence spectra

Prior the main sampling campaign, EEM fluorescence spectra of one influent and one effluent samples were analyzed to select optimal $\lambda_{ex}/\lambda_{em}$ for the further HPSEC monitoring. The EEM fluorescence spectra (Fig. 1) demonstrate intense tyrosine-like peaks B_1 and B_2 and tryptophan-like peaks T_1 and T_2, which can be related to the dissolved amino acids, free and bound to proteins, and other organic compounds with similar fluorescence properties (Fellman et

al., 2010). Tyrosine residues in proteins and peptides do not emit fluorescence in the presence of tryptophan, because the emission energy of tyrosine residues is transferred to the excitation energy of the neighboring tryptophan residues (Yamashita and Tanoue, 2003). Thus, tyrosine-like fluorescence may indicate more degraded peptide material, while tryptophan-like fluorescence may represent intact proteins and less degraded peptide material (Fellman et al., 2010).

Peaks A, C_1, C_2, and M represent fluorescence of natural humic/fulvic matter and also anthropogenic humic/fulvic-like fluorescing compounds (Carstea et al., 2016). Peaks A and C are always observed together in EEM fluorescence spectra of dissolved humic and fulvic standards isolated by International Humic Substances Society (IHSS) (Alberts and Takács, 2004). Some studies link peak A with fulvic-like compounds, whereas peaks C and M – with humic-like compounds (Chen et al., 2003). However, such interpretation seems to be rather simplified since the existing classification into humic and fulvic compounds is operational and based solubility, not on substantial differences in chemistry. In fact, the same fluorophores are found in both humic and fulvic compounds, and a clear distinction between them based uniquely on fluorescence properties is not always possible (Senesi et al., 1991).

"Red-shifted" peaks A and C_2, with emission at longer wavelengths, can be related to highly conjugated aromatic compounds of high MW, whereas "blue shifted" peaks C_1 and M, with emission at shorter wavelengths, are thought to contain compounds of lower aromaticity and lower MW (Fellman et al., 2010). Recently, peak M was suggested as indicative of mixing old and new humic/fulvic material as the result of recent microbial activity (Coble et al., 2014), since bacterial degradation is considered to be more often a source rather than a sink of humic/fulvic-like fluorescence (Coble et al., 2014; Stedmon and Markager, 2005)

Eight $\lambda_{ex}/\lambda_{em}$ were selected near maxima of EEM peaks B_1, B_2, T_1, T_2, A, C_1, and C_2 to represent variety of fluorophores and to provide high fluorescence intensity for the further HPSEC monitoring (Table 1).

3.2. Characterization of influent and effluent

Conventional surrogate parameters (BOD, COD, DOC, etc.) of whole influent and effluent samples are summarized in Supplementary material Table S1. These parameters are routinely measured 2-3 times per week to control the WWTP.

3.2.1. HPSEC fractionation

A comparison of typical HPSEC-UV-fluorescence chromatograms of influent and effluent is given in Fig. 2 and Supplementary material Fig. S1. The chromatograms exhibit fairly good resolution and provide descriptive information on the nature of wastewater DOM. A quick visual inspection of such chromatograms can directly give a rough determination of problematic fractions that are not efficiently removed during treatment (for example, fractions III and IV). Both influent and effluent demonstrated individual elution profiles, so-called fingerprints, which can assist defining type and origin of wastewater (Peuravuori and Pihlaja, 1997). These elution profiles were reproducible, although significant day-to-day variations in UVA_{254} and fluorescence intensities were observed.

For each sample, resolved peaks were combined into eight fractions, denoted I-VIII. MW of influent and effluent fractions were estimated using the calibration curve (Supplementary material Fig. S2), which is consistent with the data previously obtained by (Szabo et al., 2016) for similar conditions.

Use of calibration standards for MW estimation assumes that the standards and wastewater components behave similarly in a size-exclusion column used. Considering multicomponent nature of wastewater and diverse secondary interactions, any choice of size-exclusion standards is ambiguous. Thus, HPSEC calibration provides apparent rather than true MW. Apparent MW can be used to compare samples in a particular experiment, but should not be interpreted literally (Yan et al., 2012).

In a first approximation, compounds of high MW > 10 kDa eluted in fraction I, fraction II represented compounds of intermediate MW 3-10 kDa, fraction III consisted of compounds of MW 1-3 kDa, and fractions IV-VII combined compounds of low MW < 1 kDa. All peaks appeared

after acetone elution time 12.5 min, i.e. outside the calibration range, were deliberately combined into fraction VIII, for which estimation of MW is not possible.

High resolution archived in the range of low MW < 1 kDa can be useful for contamination tracking in groundwater recharge and water recycling, since fractions of low MW account for 67 ± 24% of the dissolved organic nitrogen in wastewater effluents, contain many precursors of disinfection by-products (Pehlivanoglu-Mantas and Sedlak, 2008), and account for most genotoxicity found in secondary effluents (Wu et al., 2010).

3.2.2. Influence of $\lambda_{ex}/\lambda_{em}$ on elution profiles

Monitoring different $\lambda_{ex}/\lambda_{em}$ belonging to the same type of fluorescence (for example, tryptophan-like T_1: 230/355 nm and T_2: 270/355 nm) resulted in noticeable variations in elution profiles (Supplementary material Fig. S3-S6). Averaged total and fractional fluorescence intensities of influent and effluent samples measured at different $\lambda_{ex}/\lambda_{em}$ are provided in Supplementary material Tables S2-S4.

Total intensity of tyrosine-like fluorescence (λ_{em} = 310 nm) at the shorter λ_{ex} = 220 nm was, on average, ~30% higher for effluent and ~10% higher for influent, compared to the longer λ_{ex} = 270 nm.

Total intensity of tryptophan-like fluorescence (λ_{em} = 355 nm) measured at the shorter λ_{ex} = 230 nm was ~10% higher for effluent, but ~25% lower for influent, compared to the longer λ_{ex} = 270 nm. These variations were mostly due to low MW fractions VI and VII. A two-fold increase in tryptophan-like fluorescence of effluent fraction VII observed at the shorter λ_{ex} is particularly interesting.

For humic/fulvic-like fluorescence shorter λ_{ex} and λ_{em}, in general, resulted in higher intensity across all influent and effluent fractions.

Effluent fraction VII, eluted around 11 min, had a very strong UV absorbance at λ < 230 nm (Supplementary material Fig. S7) that was probably caused by low MW carboxylic and amino acids formed during biological processes (Jarusutthirak and Amy, 2007). Such high UV absorbance could negatively affect accuracy of fluorescence detection for effluent fractions VI and VII due to inner filter effect at short λ_{ex} < 230 nm.

Complexation with transition metal ions, such as Fe^{3+}, should be also considered when analyzing wastewater samples, because these ions can inhibit fluorescence of humic and fulvic compounds of various MW (Cabaniss, 1992).

3.2.3. Correlations between DOC, COD, BOD, total UVA_{254}, and total fluorescence

Tyrosine-like and tryptophan-like fluorescence is often considered as a surrogate indicator of biologic activity and DOM bioavailability (Fellman et al., 2010).

Strong linear correlations (Pearson coefficient $\rho > 0.9$) were observed between DOC, COD, BOD and total UVA_{254}, total tyrosine-like, total tryptophan-like fluorescence of influent and effluent (Fig. 3 and Supplementary material Fig. S8). These correlations complement previous findings by (Bridgeman et al., 2013; Christian et al., 2017; Hudson et al., 2008; Hur and Cho, 2012) and suggest that protein-like compounds comprise a major share of fluorescing DOM in influent. The observed variations in DOC, COD, and BOD of influent reflects fluctuating patterns of diverse anthropogenic activity, including industrial discharge emissions.

At the same time, humic/fulvic-like fluorescence at $\lambda_{ex}/\lambda_{em}$ = 390/500 nm did not demonstrate significant correlations with DOC, COD, and BOD neither for influent nor for effluent (Pearson coefficient $\rho < 0.6$). It is known, that certain fractions of natural humic and fulvic compounds in wastewater derive from drinking water sources (Shon et al., 2006b). For example, (Guo et al., 2011) detected a humic/fulvic-like fraction of MW ~ 650 Da in both wastewater and tap water from the same geographical area. In Jyväskylä, drinking water is produced mainly from lake water. During the monitoring period, the rate of raw water abstraction and weather conditions, which affect quality and quantity of surface runoff water, were stable. Thus, a steady concentration of natural humic/fulvic compounds could be expected in the urban water system and, at the end, in the influent. For this reason, fluorescence at $\lambda_{ex}/\lambda_{ex}$ = 390/500 nm may be indicative of recalcitrant humic and fulvic compounds of natural origin.

Even though conventional COD and BOD measurements are required by official regulations, HPSEC-UV-fluorescence analysis can provide additional interim data to be used, for example, in early warning systems. Further research, covering a wider timespan and a larger

number of samples, is needed to determine whether the observed correlations are statistically reliable and to identify possible seasonal variations.

3.2.4. MW distributions

Percentage contributions of individual fractions to the total UVA_{254} and the total fluorescence of influent and effluent were calculated for each sampling day and afterwards were averaged. Fig. 4 and Supplementary material Fig. S9 demonstrate that, among all fractions, influent and effluent fractions VI had the strongest UV and fluorescence response (at different $\lambda_{ex}/\lambda_{em}$) and contributed to 25-30% of total UVA_{254} and 30-40% of total fluorescence. Compounds with MW < 1 kDa (fractions IV-VII combined) accounted for 60-65% of the total UVA_{254} and 50-70% of total fluorescence (at different $\lambda_{ex}/\lambda_{em}$) of influent and effluent. Among low MW fractions, fraction IV was predominantly humic/fulvic-like, fractions V and VI exhibited all types of fluorescence, whereas fraction VII was predominantly tryptophan-like with moderate humic/fulvic-like fluorescence and low tyrosine-like fluorescence.

Compounds with MW > 1 kDa (fractions I-III combined) contributed to 20-25% of the total UVA_{254} and 10-15% of the total tyrosine-like, tryptophan-like fluorescence of influent. Among them, fraction I (MW > 10 kDa) demonstrated only protein-like fluorescence, while fractions II (MW 3-10 kDa) and III (MW 1-3 kDa) exhibited also noticeable humic/fulvic-like fluorescence.

Finally, compounds eluted outside the calibration range (fraction VIII, where MW estimation is not possible) contributed to 10-15% of the total UVA_{254} and 15-20% of the total tryptophan-like and humic-fulvic-like fluorescence. Interestingly, ~40% of tyrosine-like fluorescing compounds in influent eluted outside the calibration range, while in effluent less than 20% of tyrosine-like fluorescing compounds demonstrated delayed elution. The late elution could be caused, for example, by specific interactions between wastewater components and the column material or by ion exclusion of cationic compounds (Le Coupannec et al., 2000).

Most fractions simultaneously exhibited tyrosine-like, tryptophan-like, and humic/fulvic-like fluorescence, suggesting that protein-like and humic/fulvic-like matter eluted together. Humic and fulvic compounds are known to interact with proteins and other biomolecules and form various associations including covalent bonded structures (Arenella et al., 2014; Sutton and

363 Sposito, 2005). Some humic-bound proteinaceous constituents may be more resistant to
364 biological degradation (Saadi et al., 2006). However, HPSEC-UV-fluorescence analysis does not
365 allow to discriminate whether the observed fractions consisted of individual compounds or
366 aggregates.

367 Number-averaged MWs, calculated with eq. (2) from HPSEC-UV-fluorescence
368 chromatograms, were in the range 154-238 Da for both influent and effluent (Supplementary
369 material Table S5). Weight-averaged MWs and dispersities of tyrosine-like and tryptophan-like
370 compounds were 2-4 times higher than those of humic/fulvic-like compounds.

371 The above findings support previously published data. For example, DOM in effluent from a
372 Japanese WWTP was found to have weigh-averaged MW 380-830 Da (Imai et al., 2002). Highest
373 UVA_{254} was reported for effluent fraction with MW 0.3-5 kDa (Shon et al., 2004). A bimodal
374 distribution of DOM was observed for a bench-scale activated sludge reactor fed with a synthetic
375 wastewater: 30-50% of the DOM had low MW < 1 kDa, while another 25-45% had high MW > 10
376 kDa (Jarusutthirak and Amy, 2007). Effluent from a pilot WWTP in China also exhibited a bimodal
377 MW distribution: multiple peaks with high UVA_{254} and high protein-like fluorescence at $\lambda_{ex}/\lambda_{em}$ =
378 278/353 nm were observed in the range of MW 0.1-2 kDa, and a wide peak with low UVA_{254} but
379 intense protein-like fluorescence was detected in the range of MW 10-20 kDa (Guo et al., 2011).
380 HPSEC-DOC-UVA_{254} chromatograms of effluent from a WWTP in USA displayed three segments:
381 20-60 kDa with high DOC and very low UVA_{254}; 1-20 kDa with high DOC and high UVA_{254} (with the
382 maximum around 2 kDa); and < 1 kDa with high DOC and moderate UVA_{254} (Nam and Amy,
383 2008). Effluent from a WWTP in Korea had five presumably aromatic peaks in the range of MW
384 700-2050 Da and three protein-like peaks at 480, 890, and 1690 Da, however, high MW
385 compounds were not detected (Chon et al., 2017).

386 Though detailed structural analysis, such as NMR, is rarely done for fractionated
387 wastewater, there is consensus that high MW fractions (> 10 kDa) consist of aliphatic
388 polysaccharide-like compounds and amino sugars with low aromaticity, intermediate MW
389 fractions (1-10 kDa) include various protein-like and aromatic humic/fulvic-like compounds, and
390 low MW fractions (< 1 kDa) contain organic acids, amino acids and peptides, simple sugars, and

persistent anthropogenic chemicals (Chon et al., 2017; Guo et al., 2011; Huber, 1998; Jarusutthirak and Amy, 2007; Nam and Amy, 2008).

3.2.5. UV absorbance ration index (URI)

URI (ratio of UVA_{210} to UVA_{254}) characterizes relative density of non-aromatic moieties (Her et al., 2008). Conjugated double bonds and aromatic structural elements have high UVA_{210} and high UVA_{254}, while non-aromatic moieties (amino, carbonyl, carboxyl, etc.) have high UVA_{210} and relatively low UVA_{254}. Thus, higher URI corresponds to higher relative density of non-aromatic moieties. URI helps distinguishing aromatic humic/fulvic compounds from less aromatic protein-like compounds (Shon et al., 2006a). For example, Suwannee River standard humic and fulvic acids correspondingly have URI 1.59 and 1.88 (Her et al., 2008), while for proteins of bovine serum albumin with low aromaticity URI 13.50 (Shon et al., 2006a).

Averaged URI of influent and effluent fractions and whole samples are presented in Table 2. The lowest URI (corresponding to the highest density of conjugated double bonds) was observed for influent and effluent fractions II-V and VIII indicating humic/fulvic-like nature of these fractions. High URI of influent and effluent fraction I (MW > 10 kDa) can be indicative of polysaccharides and amino sugars (Shon et al., 2006a). In contrast to humic/fulvic-like compounds and proteins, polysaccharide-like material has low UVA_{254} and low fluorescence per unit of DOC. Therefore, MW distributions obtained from HPSEC-UV_{254}-fluorescence chromatograms may underestimate high MW fractions and overestimate intermediate and low MW fractions (Her et al., 2002).

The highest URI was observed for effluent fraction VI. Considering intense tyrosine-like and tryptophan-like fluorescence, it is likely that fraction VI included considerable amounts of low MW amino acids formed during biological processes (Jarusutthirak and Amy, 2007). At the same time, co-elution of inorganic ions with strong UVA_{210}, such as nitrate, could also increase calculated URI of low MW fractions VI, VII (Szabo and Tuhkanen, 2010).

3.3. Assessment of the WWTP performance

Overall performance of the WWTP is summarized in Table 3. The values of BOD, COD, DOC, and TN removals are typical for a conventional biological treatment.

The WWTP removed half of organic carbon with conjugated double bonds, monitored by UVA_{254}. A high removal was observed for the total tyrosine-like fluorescence, followed by a satisfactory decline of the total tryptophan-like fluorescence. Reduction of the total humic/fulvic-like fluorescence did not exceed 36%, and a particularly low decline was observed at $\lambda_{ex}/\lambda_{em}$ = 390/500 nm. These results correlate well with a recent EEM-PARAFAC study by (Riopel et al., 2014), where "a large decrease (~60%) in the protein-like components was observed, followed by a smaller decrease (~28%) in the signal of the humic/fulvic-like components, and little to no change in the fulvic-like signal" before and after biological treatment of a municipal wastewater.

The observed reduction of fluorescence and UVA_{254} was lower than the reduction of BOD and COD, which suggests presence of organic compounds "invisible" for fluorescence and UV detection (for example, sugars). Apart from that, "fresh" fluorescing material formed during microbial metabolism (de novo synthesis) could additionally contribute to fluorescence signal of effluent. Moreover, certain organic compounds present in influent and capable of fluorescence quenching could be degraded during WWTP treatment (Saadi et al., 2006).

URI of whole wastewater samples increased almost three-fold during the treatment (Table 2) pointing out that, overall, humification did not occur (Maizel and Remucal, 2017). At the same time, the treatment noticeably increased dispersity of protein-like compounds (Supplementary material Table S5), which can be explained in terms of high MW of extracellular polymeric substances secreted by microorganisms in activated sludge.

Analysis of HPSEC-UV-fluorescence chromatograms allows tracking individual tyrosine-like, tryptophan-like, and humic/fulvic-like fractions. Observed removal efficiencies considerably varied for fractions of different MW (Supplementary material Table S6). Fractions IV and V (MW < 1 kDa) demonstrated recalcitrant behavior with removal efficiencies significantly below 50% for UVA_{254} and fluorescence at different $\lambda_{ex}/\lambda_{em}$ and especially for humic/fulvic-like fluorescence. The highest removal efficiencies (above 80%) were observed for fraction I (MW > 10 kDa). Fractions III-VIII, in general, had significantly higher removal efficiencies for tyrosine-like and tryptophan-like fluorescence than for humic/fulvic-like fluorescence. Slight increase of humic/fulvic-like

fluorescence of fractions V-VII observed at $\lambda_{ex}/\lambda_{em}$ = 390/500 nm may indicate formation of new fluorescing material, for example, as result of sludge digestion.

According to the calculated URI values (Table 3), aromatic character of wastewater fractions II-V, VII, and VIII slightly increased during the biological treatment due to less efficient removal of humic/fulvic-like compounds compared to protein-like compounds. Formation of non-aromatic microbial products of high and low MW, probably, caused the noticeable increase of URI of fractions I and VI.

4. Conclusions

Comparative interpretation of HPSEC-UV-fluorescence chromatograms of wastewater influents and effluents can shed light on the behavior of protein-like and humic/fulvic-like fractions in WWTPs and provide a deeper understanding of anthropogenic organic matter in urban hydrological cycle.

HPSEC-UV-fluorescence analysis of municipal wastewater using the proposed method revealed seven fractions within the calibration range. Compounds of low MW < 1 kDa were resolved into four fractions and accounted for 60-70% of total UVA_{254} and 70-80% of total fluorescence.

Most fractions were mixtures of protein-like and humic/fulvic-like matter. The fraction of high MW > 10 kDa had low fluorescence and low UVA_{254}, exhibiting non-aromatic character.

High removal efficiencies were observed for most tyrosine-like and tryptophan-like fractions. At the same time, low MW humic/fulvic-like fractions, especially those fluorescing at $\lambda_{ex}/\lambda_{em}$ = 390/500 nm, demonstrated recalcitrant behavior in the WWTP.

Since composition of wastewater can significantly differ, preliminary selection of optimal $\lambda_{ex}/\lambda_{ex}$ for fluorescence monitoring should be done individually for each WWTP considering possible seasonal variations. For this purpose, EEM fluorescence spectroscopy can be recommended. This study focused on fluorescing and UV absorbing wastewater fractions. Thus, certain categories of organic compounds (for example, polysaccharides) were not covered.

HPSEC analysis of complex water matrices, such as wastewater, requires minimal sample preparation and allows collecting an extensive dataset within short time (~30 min per analysis)

using multiple detectors connected in a series. Although unambiguous interpretation of UV and fluorescence spectra is challenging, the proposed HPSEC-UV-fluorescence approach is promising for fingerprinting and tracking specific wastewater fractions and advanced monitoring of WWTP performance.

Acknowledgments

The first author sincerely appreciates the financial support of Ekokem Oy for a scholarship. Jyväskylän Seudun Puhdistamo Oy and Nablabs Oy are gratefully acknowledged for fruitful cooperation and assistance with the wastewater sampling. The help of laboratory technicians Mervi Koistinen and Leena Siitonen is greatly appreciated. Also, the authors wish to thank two anonymous reviewers for their constructive comments.

Appendix A. Supplementary material

Supplementary material related to this article can be found online at

References

Abbt-Braun, G., Lankes, U., Frimmel, F.H., 2004. Structural characterization of aquatic humic substances – The need for a multiple method approach. Aquat. Sci. - Res. Boundaries 66, 151–170. https://doi.org/10.1007/s00027-004-0711-z

Alberts, J.J., Takács, M., 2004. Total luminescence spectra of IHSS standard and reference fulvic acids, humic acids and natural organic matter: comparison of aquatic and terrestrial source terms. Org. Geochem. 35, 243–256. https://doi.org/10.1016/j.orggeochem.2003.11.007

Arenella, M., Giagnoni, L., Masciandaro, G., Ceccanti, B., Nannipieri, P., Renella, G., 2014. Interactions between proteins and humic substances affect protein identification by mass spectrometry. Biol. Fertil. Soils 50, 447–454. https://doi.org/10.1007/s00374-013-0860-0

Bridgeman, J., Baker, A., Carliell-Marquet, C., Carstea, E., 2013. Determination of changes in wastewater quality through a treatment works using fluorescence spectroscopy. Environ. Technol. 34, 3069–3077. https://doi.org/10.1080/09593330.2013.803131

501 Cabaniss, S.E., 1992. Synchronous fluorescence spectra of metal-fulvic acid complexes. Environ.
502 Sci. Technol. 26, 1133–1139. https://doi.org/10.1021/es50002a018
503 Carstea, E.M., Bridgeman, J., Baker, A., Reynolds, D.M., 2016. Fluorescence spectroscopy for
504 wastewater monitoring: a review. Water Res. 95, 205–219.
505 https://doi.org/10.1016/j.watres.2016.03.021
506 Chen, W., Westerhoff, P., Leenheer, J.A., Booksh, K., 2003. Fluorescence excitation−emission
507 matrix regional integration to quantify spectra for dissolved organic matter. Environ. Sci.
508 Technol. 37, 5701–5710. https://doi.org/10.1021/es034354c
509 Chon, Kangmin, Chon, Kyongmi, Cho, J., 2017. Characterization of size fractionated dissolved
510 organic matter from river water and wastewater effluent using preparative high
511 performance size exclusion chromatography. Org. Geochem. 103, 105–112.
512 https://doi.org/10.1016/j.orggeochem.2016.11.003
513 Choudhry, G.G., 1983. Humic substances. Part III. Sorptive interactions with environmental
514 chemicals. Toxicol. Environ. Chem. 6, 127–171.
515 https://doi.org/10.1080/02772248309357000
516 Christian, E., Batista, J.R., Gerrity, D., 2017. Use of COD, TOC, and fluorescence spectroscopy to
517 estimate BOD in wastewater. Water Environ. Res. 89, 168–177.
518 https://doi.org/10.2175/106143016X14504669768976
519 Coble, P.G., Lead, J., Baker, A., Reynolds, D.M., Spencer, R.G.M. (Eds.), 2014. Aquatic Organic
520 Matter Fluorescence, Cambridge Environmental Chemistry Series. Cambridge University
521 Press, Cambridge. https://doi.org/10.1017/CBO9781139045452
522 Directive, 2013. Directive 2013/39/EU of the European Parliament and of the Council of 12
523 August 2013 amending Directives 2000/60/EC and 2008/105/EC as regards priority
524 substances in the field of water policy. Off. J. Eur. Union L 226, 1–17.
525 Directive, 1991. Council Directive of 21 May 1991 concerning urban waste water treatment
526 (91/271/EEC). Off. J. Eur. Communities L 135, 40–52.

527 European Commission, 2017. Ninth Report on the implementation status and the programmes
528 for implementation (as required by Article 17) of Council Directive 91/271/EEC
529 concerning urban waste water treatment. Brussels.
530 Feitelson, J., 1964. On the mechanism of fluorescence quenching. Tyrosine and similar
531 compounds. J. Phys. Chem. 68, 391–397. https://doi.org/10.1021/j100784a033
532 Fellman, J.B., Hood, E., Spencer, R.G.M., 2010. Fluorescence spectroscopy opens new windows
533 into dissolved organic matter dynamics in freshwater ecosystems: a review. Limnol.
534 Oceanogr. 55, 2452–2462. https://doi.org/10.4319/lo.2010.55.6.2452
535 Guo, Jin, Peng, Y., Guo, Jianhua, Ma, J., Wang, W., Wang, B., 2011. Dissolved organic matter in
536 biologically treated sewage effluent (BTSE): characteristics and comparison. Desalination
537 278, 365–372. https://doi.org/10.1016/j.desal.2011.05.057
538 Henderson, R.K., Baker, A., Murphy, K.R., Hambly, A., Stuetz, R.M., Khan, S.J., 2009.
539 Fluorescence as a potential monitoring tool for recycled water systems: a review. Water
540 Res. 43, 863–881. https://doi.org/10.1016/j.watres.2008.11.027
541 Her, N., Amy, G., Foss, D., Cho, J., 2002. Variations of molecular weight estimation by HP-size
542 exclusion chromatography with UVA versus online DOC detection. Environ. Sci. Technol.
543 36, 3393–3399. https://doi.org/10.1021/es015649y
544 Her, N., Amy, G., McKnight, D., Sohn, J., Yoon, Y., 2003. Characterization of DOM as a function of
545 MW by fluorescence EEM and HPLC-SEC using UVA, DOC, and fluorescence detection.
546 Water Res. 37, 4295–4303. https://doi.org/10.1016/S0043-1354(03)00317-8
547 Her, N., Amy, G., Sohn, J., Gunten, U., 2008. UV absorbance ratio index with size exclusion
548 chromatography (URI-SEC) as an NOM property indicator. J. Water Supply Res. Technol.-
549 Aqua 57, 35–44. https://doi.org/10.2166/aqua.2008.029
550 Huber, S.A., 1998. Evidence for membrane fouling by specific TOC constituents. Desalination
551 119, 229–234. https://doi.org/10.1016/S0011-9164(98)00162-3
552 Hudson, N., Baker, A., Ward, D., Reynolds, D.M., Brunsdon, C., Carliell-Marquet, C., Browning, S.,
553 2008. Can fluorescence spectrometry be used as a surrogate for the Biochemical Oxygen

554 Demand (BOD) test in water quality assessment? An example from South West England.
555 Sci. Total Environ. 391, 149–158. https://doi.org/10.1016/j.scitotenv.2007.10.054
556 Hur, J., Cho, J., 2012. Prediction of BOD, COD, and total nitrogen concentrations in a typical
557 urban river using a fluorescence excitation-emission matrix with PARAFAC and UV
558 absorption indices. Sensors 12, 972–986. https://doi.org/10.3390/s120100972
559 Imai, A., Fukushima, T., Matsushige, K., Kim, Y.-H., Choi, K., 2002. Characterization of dissolved
560 organic matter in effluents from wastewater treatment plants. Water Res. 36, 859–870.
561 https://doi.org/10.1016/S0043-1354(01)00283-4
562 Ishii, S.K.L., Boyer, T.H., 2012. Behavior of reoccurring PARAFAC components in fluorescent
563 dissolved organic matter in natural and engineered systems: a critical review. Environ.
564 Sci. Technol. 46, 2006–2017. https://doi.org/10.1021/es2043504
565 Jarusutthirak, C., Amy, G., 2007. Understanding soluble microbial products (SMP) as a
566 component of effluent organic matter (EfOM). Water Res. 41, 2787–2793.
567 https://doi.org/10.1016/j.watres.2007.03.005
568 Kothawala, D.N., Murphy, K.R., Stedmon, C.A., Weyhenmeyer, G.A., Tranvik, L.J., 2013. Inner filter
569 correction of dissolved organic matter fluorescence: correction of inner filter effects.
570 Limnol. Oceanogr. Methods 11, 616–630. https://doi.org/10.4319/lom.2013.11.616
571 Lawaetz, A.J., Stedmon, C.A., 2009. Fluorescence intensity calibration using the Raman scatter
572 peak of water. Appl. Spectrosc. 63, 936–940.
573 https://doi.org/10.1366/000370209788964548
574 Le Coupannec, F., Morin, D., Sire, O., Péron, J.-J., 2000. Influence of secondary interactions on
575 high performance size exclusion chromatography. Application to the fractionation of
576 landfill leachates. Analusis 28, 543–549. https://doi.org/10.1051/analusis:2000169
577 Li, W.-T., Chen, S.-Y., Xu, Z.-X., Li, Y., Shuang, C.-D., Li, A.-M., 2014. Characterization of dissolved
578 organic matter in municipal wastewater using fluorescence PARAFAC analysis and
579 chromatography multi-excitation/emission scan: a comparative study. Environ. Sci.
580 Technol. 48, 2603–2609. https://doi.org/10.1021/es404624q

581 Li, W.-T., Majewsky, M., Abbt-Braun, G., Horn, H., Jin, J., Li, Q., Zhou, Q., Li, A.-M., 2016.
582 Application of portable online LED UV fluorescence sensor to predict the degradation of
583 dissolved organic matter and trace organic contaminants during ozonation. Water Res.
584 101, 262–271. https://doi.org/10.1016/j.watres.2016.05.090
585 Maizel, A.C., Remucal, C.K., 2017. The effect of advanced secondary municipal wastewater
586 treatment on the molecular composition of dissolved organic matter. Water Res. 122,
587 42–52. https://doi.org/10.1016/j.watres.2017.05.055
588 Mesquita, D.P., Quintelas, C., Amaral, A.L., Ferreira, E.C., 2017. Monitoring biological wastewater
589 treatment processes: recent advances in spectroscopy applications. Rev. Environ. Sci.
590 Biotechnol. 16, 395–424. https://doi.org/10.1007/s11157-017-9439-9
591 Michael-Kordatou, I., Michael, C., Duan, X., He, X., Dionysiou, D.D., Mills, M.A., Fatta-Kassinos, D.,
592 2015. Dissolved effluent organic matter: characteristics and potential implications in
593 wastewater treatment and reuse applications. Water Res. 77, 213–248.
594 https://doi.org/10.1016/j.watres.2015.03.011
595 Nam, S.-N., Amy, G., 2008. Differentiation of wastewater effluent organic matter (EfOM) from
596 natural organic matter (NOM) using multiple analytical techniques. Water Sci. Technol.
597 57, 1009–1015. https://doi.org/10.2166/wst.2008.165
598 Pehlivanoglu-Mantas, E., Sedlak, D.L., 2008. Measurement of dissolved organic nitrogen forms in
599 wastewater effluents: Concentrations, size distribution and NDMA formation potential.
600 Water Res. 42, 3890–3898. https://doi.org/10.1016/j.watres.2008.05.017
601 Peuravuori, J., Pihlaja, K., 1997. Molecular size distribution and spectroscopic properties of
602 aquatic humic substances. Anal. Chim. Acta 337, 133–149.
603 https://doi.org/10.1016/S0003-2670(96)00412-6
604 Riopel, R., Caron, F., Siemann, S., 2014. Fluorescence characterization of natural organic matter
605 at a Northern Ontario wastewater treatment plant. Water. Air. Soil Pollut. 225.
606 https://doi.org/10.1007/s11270-014-2126-3

607 Saadi, I., Borisover, M., Armon, R., Laor, Y., 2006. Monitoring of effluent DOM biodegradation
608 using fluorescence, UV and DOC measurements. Chemosphere 63, 530–539.
609 https://doi.org/10.1016/j.chemosphere.2005.07.075
610 Senesi, N., Miano, T.M., Provenzano, M.R., Brunetti, G., 1991. Characterization, differentiation,
611 and classification of humic substances by fluorescence spectroscopy. Soil Sci. 152, 259–
612 271.
613 Shon, H.-K., Kim, S.-H., Erdei, L., Vigneswaran, S., 2006a. Analytical methods of size distribution
614 for organic matter in water and wastewater. Korean J. Chem. Eng. 23, 581–591.
615 https://doi.org/10.1007/BF02706798
616 Shon, H.-K., Vigneswaran, S., Kim, I.S., Cho, J., Ngo, H.., 2004. The effect of pretreatment to
617 ultrafiltration of biologically treated sewage effluent: a detailed effluent organic matter
618 (EfOM) characterization. Water Res. 38, 1933–1939.
619 https://doi.org/10.1016/j.watres.2004.01.015
620 Shon, H.-K., Vigneswaran, S., Snyder, S.A., 2006b. Effluent organic matter (EfOM) in wastewater:
621 constituents, effects, and treatment. Crit. Rev. Environ. Sci. Technol. 36, 327–374.
622 https://doi.org/10.1080/10643380600580011
623 Sillanpää, M., Matilainen, A., Lahtinen, T., 2015. Characterization of NOM, in: Natural Organic
624 Matter in Water. Elsevier, pp. 17–53. https://doi.org/10.1016/B978-0-12-801503-
625 2.00002-1
626 Specht, C.H., Frimmel, F.H., 2000. Specific interactions of organic substances in size-exclusion
627 chromatography. Environ. Sci. Technol. 34, 2361–2366.
628 https://doi.org/10.1021/es991034d
629 Stedmon, C.A., Markager, S., 2005. Tracing the production and degradation of autochthonous
630 fractions of dissolved organic matter by fluorescence analysis. Limnol. Oceanogr. 50,
631 1415–1426. https://doi.org/10.4319/lo.2005.50.5.1415
632 Sutton, R., Sposito, G., 2005. Molecular structure in soil humic substances: the new view.
633 Environ. Sci. Technol. 39, 9009–9015. https://doi.org/10.1021/es050778q

634 Szabo, H.M., Lepistö, R., Tuhkanen, T., 2016. HPLC-SEC: a new approach to characterise complex
635 wastewater effluents. Int. J. Environ. Anal. Chem. 96, 257–270.
636 https://doi.org/10.1080/03067319.2016.1150463
637 Szabo, H.M., Tuhkanen, T., 2010. The application of HPLC–SEC for the simultaneous
638 characterization of NOM and nitrate in well waters. Chemosphere 80, 779–786.
639 https://doi.org/10.1016/j.chemosphere.2010.05.007
640 Wu, Q.-Y., Hu, H.-Y., Zhao, X., Li, Y., 2010. Effects of chlorination on the properties of dissolved
641 organic matter and its genotoxicity in secondary sewage effluent under two different
642 ammonium concentrations. Chemosphere 80, 941–946.
643 https://doi.org/10.1016/j.chemosphere.2010.05.005
644 Yamashita, Y., Tanoue, E., 2003. Chemical characterization of protein-like fluorophores in DOM in
645 relation to aromatic amino acids. Mar. Chem. 82, 255–271.
646 https://doi.org/10.1016/S0304-4203(03)00073-2
647 Yan, M., Korshin, G., Wang, D., Cai, Z., 2012. Characterization of dissolved organic matter using
648 high-performance liquid chromatography (HPLC)–size exclusion chromatography (SEC)
649 with a multiple wavelength absorbance detector. Chemosphere 87, 879–885.
650 https://doi.org/10.1016/j.chemosphere.2012.01.029
651 Yang, L., Hur, J., Zhuang, W., 2015. Occurrence and behaviors of fluorescence EEM-PARAFAC
652 components in drinking water and wastewater treatment systems and their applications:
653 a review. Environ. Sci. Pollut. Res. 22, 6500–6510. https://doi.org/10.1007/s11356-
654 015-4214-3
655

Figure 1.

EEM fluorescence spectra of (a) influent and (b) effluent after fivefold dilution. DOC before dilution: 58.0 mgC L^{-1} (influent) and 19.6 mgC L^{-1} (effluent). Sampling date: March 19, 2017.
(2-column fitting image)

Figure 2.

Normalized HPSEC chromatograms of influent and effluent with (a)-(c) fluorescence and (d) UV detection. DOC 89.2 mgC L^{-1} (influent) and 27.2 mgC L^{-1} (effluent). Additional horizontal axis at the bottom provides estimation of MW. Bar diagrams on the right show averaged removal efficiencies for individual fractions and total signals, mean ± SD (n = 10). Sampling date: March 30, 2017. Additional HPSEC-fluorescence chromatograms are given in Supplementary material Fig. S1.
(2-column fitting image)

Figure 3.

Correlations between DOC, COD, BOD and total UVA_{254}, total tyrosine-like, and total tryptophan-like fluorescence of influent (triangles) and effluent (circles) samples. ρ is Pearson correlation coefficient. Linear equations were obtained using robust regression (MATLAB function robustfit). Number of influent/effluent pairs: 25 for DOC, 17 for COD and BOD. For additional fluorescence $\lambda_{ex}/\lambda_{em}$ refer to Supplementary material Fig. S8.
(2-column fitting image)

Figure 4.

Percentage contribution of individual fractions into (a)-(c) total fluorescence and (d) total UVA_{254} of influent and effluent. Mean ± SD (n = 10). For additional fluorescence $\lambda_{ex}/\lambda_{em}$ refer to Supplementary material Fig. S9.
(2-column fitting image)

Table 1. $\lambda_{ex}/\lambda_{em}$ selected for the HPSEC-fluorescence monitoring and corresponding EEM peaks.

Fluorescence type	EEM peak	$\lambda_{ex}/\lambda_{em}$ (nm)
Tyrosine-like	B_1	220/310
	B_2	270/310
Tryptophan-like	T_2	230/355
	T_1	270/355
Humic/fulvic-like	A	240/440
	A	270/500
	C_1	330/425
	C_2	390/500

Table 2. URI of influent and effluent fractions and whole samples. Mean ± SD (*n* = 10).

Fraction	Influent	Effluent
I	6.1 ± 0.8	15.1 ± 2.7
II	3.0 ± 0.4	2.7 ± 0.3
III	2.6 ± 0.4	2.3 ± 0.3
IV	2.9 ± 0.5	2.5 ± 0.3
V	3.2 ± 0.8	2.9 ± 0.6
VI	3.7 ± 0.4	28.6 ± 4.1
VII	3.9 ± 0.3	3.1 ± 0.4
VIII	2.9 ± 0.4	2.6 ± 0.5
Whole sample	3.4 ± 0.4	10.0 ± 1.1

Table 3. Overall efficiency of the WWTP. Mean ± SD.

Parameter		**Removal (%)**
BOD		97 ± 1
COD		93 ± 2
DOC		71 ± 7
TN		24 ± 7
Total UVA_{254}		50 ± 6
Total fluorescence:		
Tyrosine-like	B_1: 220/310 nm	80 ± 5
	B_2: 270/310 nm	83 ± 5
Tryptophan-like	T_1: 230/355 nm	55 ± 5
	T_2: 270/355 nm	70 ± 3
Humic/fulvic-like	A: 240/440 nm	36 ± 4
	A: 270/500 nm	32 ± 2
	C_1: 330/425 nm	25 ± 4
	C_2: 390/500 nm	7 ± 3

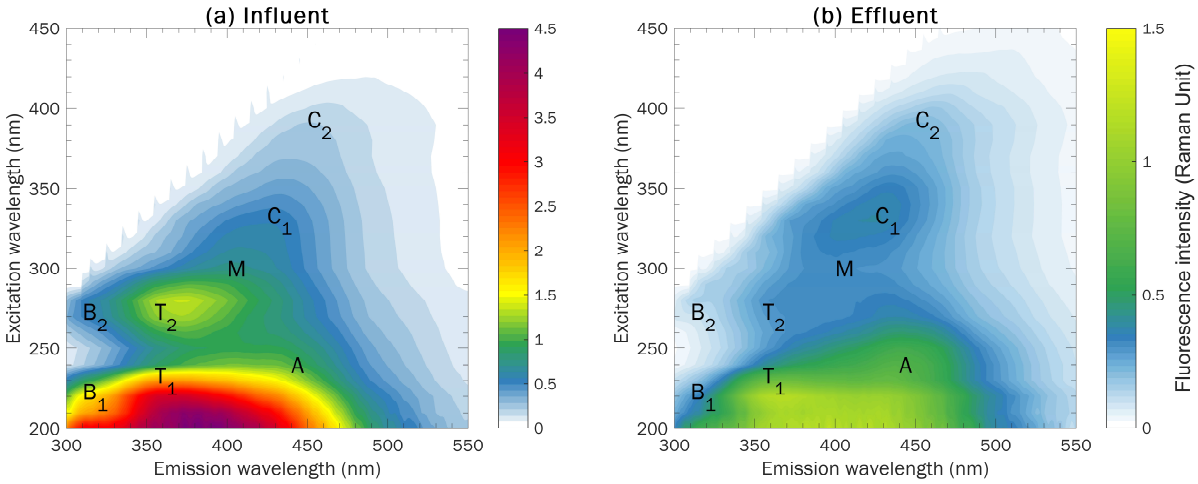

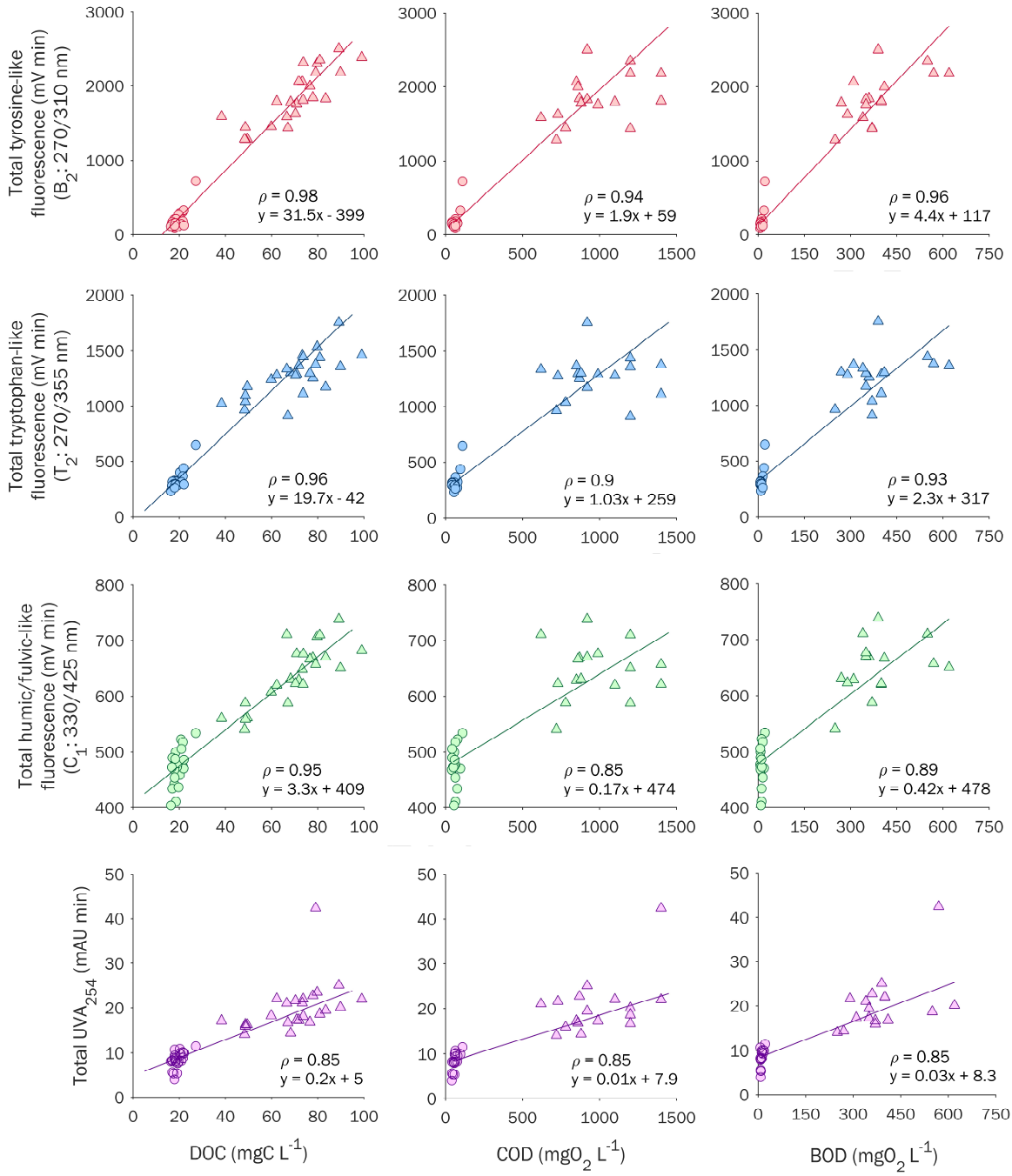
Total tyrosine-like fluorescence (mV min) (B_2: 270/310 nm)
ρ = 0.98
y = 31.5x - 399
ρ = 0.94
y = 1.9x + 59
ρ = 0.96
y = 4.4x + 117
Total tryptophan-like fluorescence (mV min) (T_2: 270/355 nm)
ρ = 0.96
y = 19.7x - 42
ρ = 0.9
y = 1.03x + 259
ρ = 0.93
y = 2.3x + 317
Total humic/fulvic-like fluorescence (mV min) (C_1: 330/425 nm)
ρ = 0.95
y = 3.3x + 409
ρ = 0.85
y = 0.17x + 474
ρ = 0.89
y = 0.42x + 478
Total UVA_{254} (mAU min)
ρ = 0.85
y = 0.2x + 5
ρ = 0.85
y = 0.01x + 7.9
ρ = 0.85
y = 0.03x + 8.3
DOC (mgC L^{-1})
COD (mgO_2 L^{-1})
BOD (mgO_2 L^{-1})

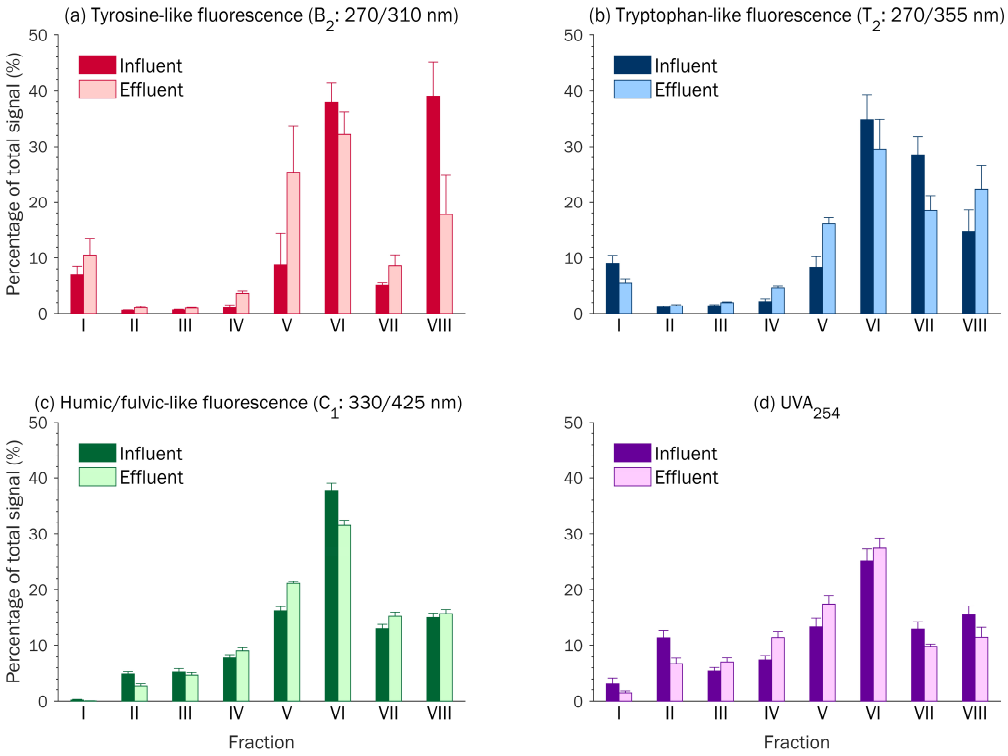

- Low MW compounds accounted for ~60% of UVA_{254} and ~70% of wastewater fluorescence.
- Conventional biological treatment reduced total UVA_{254} by ~50%.
- In total, 55-83% of protein-like and < 36% of humic-like fluorescence was removed.
- Recalcitrant humic-like fractions were detected at $\lambda_{ex}/\lambda_{em}$ = 390/500 nm.
- Linear correlations between BOD, COD, DOC and fluorescence, UVA_{254} were observed.